

First Observation of $\eta(1405)$ Decays into $f_0(980)\pi^0$

M. Ablikim,¹ M. N. Achasov,⁵ D. Alberto,⁴¹ D. J. Ambrose,³⁸ F. F. An,¹ Q. An,³⁹ Z. H. An,¹ J. Z. Bai,¹
 R. B. F. Baldini Ferroli,¹⁷ Y. Ban,²⁵ J. Becker,² N. Berger,¹ M. B. Bertani,¹⁷ J. M. Bian,¹ E. Boger,^{18,*} O. Bondarenko,¹⁹
 I. Boyko,¹⁸ R. A. Briere,³ V. Bytev,¹⁸ X. Cai,¹ A. C. Calcaterra,¹⁷ G. F. Cao,¹ J. F. Chang,¹ G. Chelkov,^{18,*} G. Chen,¹
 H. S. Chen,¹ J. C. Chen,¹ M. L. Chen,¹ S. J. Chen,²³ Y. Chen,¹ Y. B. Chen,¹ H. P. Cheng,¹³ Y. P. Chu,¹
 D. Cronin-Hennessy,³⁷ H. L. Dai,¹ J. P. Dai,¹ D. Dedovich,¹⁸ Z. Y. Deng,¹ I. Denysenko,^{18,†} M. Destefanis,⁴¹
 W. L. Ding Ding,²⁷ Y. Ding,²¹ L. Y. Dong,¹ M. Y. Dong,¹ S. X. Du,⁴⁴ J. Fang,¹ S. S. Fang,¹ C. Q. Feng,³⁹ C. D. Fu,¹
 J. L. Fu,²³ Y. Gao,³⁴ C. Geng,³⁹ K. Goetzen,⁷ W. X. Gong,¹ M. Greco,⁴¹ M. H. Gu,¹ Y. T. Gu,⁹ Y. H. Guan,⁶ A. Q. Guo,²⁴
 L. B. Guo,²² Y. P. Guo,²⁴ Y. L. Han,¹ X. Q. Hao,¹ F. A. Harris,³⁶ K. L. He,¹ M. He,¹ Z. Y. He,²⁴ Y. K. Heng,¹ Z. L. Hou,¹
 H. M. Hu,¹ J. F. Hu,⁶ T. Hu,¹ B. Huang,¹ G. M. Huang,¹⁴ J. S. Huang,¹¹ X. T. Huang,²⁷ Y. P. Huang,¹ T. Hussain,⁴⁰ C. S. Ji,³⁹
 Q. Ji,¹ X. B. Ji,¹ X. L. Ji,¹ L. K. Jia,¹ L. L. Jiang,¹ X. S. Jiang,¹ J. B. Jiao,²⁷ Z. Jiao,¹³ D. P. Jin,¹ S. Jin,¹ F. F. Jing,³⁴
 N. Kalantar-Nayestanaki,¹⁹ M. Kavatsyuk,¹⁹ W. Kuehn,³⁵ W. Lai,¹ J. S. Lange,³⁵ J. K. C. Leung,³³ C. H. Li,¹ Cheng Li,³⁹
 Cui Li,³⁹ D. M. Li,⁴⁴ F. Li,¹ G. Li,¹ H. B. Li,¹ J. C. Li,¹ K. Li,¹⁰ Lei Li,¹ N. B. Li,²² Q. J. Li,¹ S. L. Li,¹ W. D. Li,¹ W. G. Li,¹
 X. L. Li,²⁷ X. N. Li,¹ X. Q. Li,²⁴ X. R. Li,²⁶ Z. B. Li,³¹ H. Liang,³⁹ Y. F. Liang,²⁹ Y. T. Liang,³⁵ G. R. Liao,³⁴ X. T. Liao,¹
 B. J. Liu,³² C. L. Liu,³ C. X. Liu,¹ C. Y. Liu,¹ F. H. Liu,²⁸ Fang Liu,¹ Feng Liu,¹⁴ H. Liu,¹ H. B. Liu,⁶ H. H. Liu,¹²
 H. M. Liu,¹ H. W. Liu,¹ J. P. Liu,⁴² K. Liu,²⁵ K. Liu,⁶ K. Y. Liu,²¹ Q. Liu,³⁶ S. B. Liu,³⁹ X. Liu,²⁰ X. H. Liu,¹ Y. B. Liu,²⁴
 Yong Liu,¹ Z. A. Liu,¹ Zhiqiang Liu,¹ Zhiqing Liu,¹ H. Loehner,¹⁹ G. R. Lu,¹¹ H. J. Lu,¹³ J. G. Lu,¹ Q. W. Lu,²⁸ X. R. Lu,⁶
 Y. P. Lu,¹ C. L. Luo,²² M. X. Luo,⁴³ T. Luo,³⁶ X. L. Luo,¹ M. Lv,¹ C. L. Ma,⁶ F. C. Ma,²¹ H. L. Ma,¹ Q. M. Ma,¹ S. Ma,¹
 T. Ma,¹ X. Y. Ma,¹ M. Maggiora,⁴¹ Q. A. Malik,⁴⁰ H. Mao,¹ Y. J. Mao,²⁵ Z. P. Mao,¹ J. G. Messchendorp,¹⁹ J. Min,¹
 T. J. Min,¹ R. E. Mitchell,¹⁶ X. H. Mo,¹ N. Yu. Muchnoi,⁵ Y. Nefedov,¹⁸ I. B. Nikolaev,⁵ Z. Ning,¹ S. L. Olsen,²⁶
 Q. Ouyang,¹ S. P. Pacetti,^{17,‡} J. W. Park,²⁶ M. Pelizaeus,³⁶ K. Peters,⁷ J. L. Ping,²² R. G. Ping,¹ R. Poling,³⁷ C. S. J. Pun,³³
 M. Qi,²³ S. Qian,¹ C. F. Qiao,⁶ X. S. Qin,¹ J. F. Qiu,¹ K. H. Rashid,⁴⁰ G. Rong,¹ X. D. Ruan,⁹ A. Sarantsev,^{18,§} J. Schulze,²
 M. Shao,³⁹ C. P. Shen,^{36,||} X. Y. Shen,¹ H. Y. Sheng,¹ M. R. Shepherd,¹⁶ X. Y. Song,¹ S. Spataro,⁴¹ B. Spruck,³⁵ D. H. Sun,¹
 G. X. Sun,¹ J. F. Sun,¹¹ S. S. Sun,¹ X. D. Sun,¹ Y. J. Sun,³⁹ Y. Z. Sun,¹ Z. J. Sun,¹ Z. T. Sun,³⁹ C. J. Tang,²⁹ X. Tang,¹
 E. H. Thorndike,³⁸ H. L. Tian,¹ D. Toth,³⁷ G. S. Varner,³⁶ X. Wan,¹ B. Wang,⁹ B. Q. Wang,²⁵ K. Wang,¹ L. L. Wang,⁴
 L. S. Wang,¹ M. Wang,²⁷ P. Wang,¹ P. L. Wang,¹ Q. Wang,¹ Q. J. Wang,¹ S. G. Wang,²⁵ X. F. Wang,¹¹ X. L. Wang,³⁹
 Y. D. Wang,³⁹ Y. F. Wang,¹ Y. Q. Wang,²⁷ Z. Wang,¹ Z. G. Wang,¹ Z. Y. Wang,¹ D. H. Wei,⁸ Q. G. Wen,³⁹ S. P. Wen,¹
 U. Wiedner,² L. H. Wu,¹ N. Wu,¹ W. Wu,²⁴ Z. Wu,¹ Z. J. Xiao,²² Y. G. Xie,¹ Q. L. Xiu,¹ G. F. Xu,¹ G. M. Xu,²⁵ H. Xu,¹
 Q. J. Xu,¹⁰ X. P. Xu,³⁰ Y. Xu,²⁴ Z. R. Xu,³⁹ Z. Xue,¹ L. Yan,³⁹ W. B. Yan,³⁹ Y. H. Yan,¹⁵ H. X. Yang,¹ T. Yang,⁹ Y. Yang,¹⁴
 Y. X. Yang,⁸ H. Ye,¹ M. Ye,¹ M. H. Ye,⁴ B. X. Yu,¹ C. X. Yu,²⁴ S. P. Yu,²⁷ C. Z. Yuan,¹ W. L. Yuan,²² Y. Yuan,¹ A. A. Zafar,⁴⁰
 A. Z. Zallo,¹⁷ Y. Zeng,¹⁵ B. X. Zhang,¹ B. Y. Zhang,¹ C. C. Zhang,¹ D. H. Zhang,¹ H. H. Zhang,³¹ H. Y. Zhang,¹ J. Zhang,²²
 J. Q. Zhang,¹ J. W. Zhang,¹ J. Y. Zhang,¹ J. Z. Zhang,¹ L. Zhang,²³ S. H. Zhang,¹ T. R. Zhang,²² X. J. Zhang,¹ X. Y. Zhang,²⁷
 Y. Zhang,¹ Y. H. Zhang,¹ Y. S. Zhang,⁹ Z. P. Zhang,³⁹ Z. Y. Zhang,⁴² G. Zhao,¹ H. S. Zhao,¹ Jingwei Zhao,¹ Lei Zhao,³⁹
 Ling Zhao,¹ M. G. Zhao,²⁴ Q. Zhao,¹ S. J. Zhao,⁴⁴ T. C. Zhao,¹ X. H. Zhao,²³ Y. B. Zhao,¹ Z. G. Zhao,³⁹
 A. Zhemchugov,^{18,*} B. Zheng,¹ J. P. Zheng,¹ Y. H. Zheng,⁶ Z. P. Zheng,¹ B. Zhong,¹ J. Zhong,² L. Zhou,¹ X. K. Zhou,⁶
 X. R. Zhou,³⁹ C. Zhu,¹ K. Zhu,¹ K. J. Zhu,¹ S. H. Zhu,¹ X. L. Zhu,³⁴ X. W. Zhu,¹ Y. S. Zhu,¹ Z. A. Zhu,¹ J. Zhuang,¹
 B. S. Zou,¹ J. H. Zou,¹ and J. X. Zuo¹

(BESIII Collaboration)

¹Institute of High Energy Physics, Beijing 100049, People's Republic of China

²Bochum Ruhr-University, 44780 Bochum, Germany

³Carnegie Mellon University, Pittsburgh, Pennsylvania 15213, USA

⁴China Center of Advanced Science and Technology, Beijing 100190, People's Republic of China

⁵G. I. Budker Institute of Nuclear Physics SB RAS (BINP), Novosibirsk 630090, Russia

⁶Graduate University of Chinese Academy of Sciences, Beijing 100049, People's Republic of China

⁷GSI Helmholtzcentre for Heavy Ion Research GmbH, D-64291 Darmstadt, Germany

⁸Guangxi Normal University, Guilin 541004, People's Republic of China

⁹Guangxi University, Nanning, 530004, People's Republic of China

¹⁰Hangzhou Normal University, XueLin Jie 16, Xiasha Higher Education Zone, Hangzhou, 310036

¹¹Henan Normal University, Xinxiang 453007, People's Republic of China

- ¹²Henan University of Science and Technology, Luoyang 471003, People's Republic of China
¹³Huangshan College, Huangshan 245000, People's Republic of China
¹⁴Huazhong Normal University, Wuhan 430079, People's Republic of China
¹⁵Hunan University, Changsha 410082, People's Republic of China
¹⁶Indiana University, Bloomington, Indiana 47405, USA
¹⁷INFN Laboratori Nazionali di Frascati, Frascati, Italy
¹⁸Joint Institute for Nuclear Research, Dubna, Russia
¹⁹KVI/University of Groningen, AA Groningen, The Netherlands
²⁰Lanzhou University, Lanzhou 730000, People's Republic of China
²¹Liaoning University, Shenyang 110036, People's Republic of China
²²Nanjing Normal University, Nanjing 210046, People's Republic of China
²³Nanjing University, Nanjing 210093, People's Republic of China
²⁴Nankai University, Tianjin 300071, People's Republic of China
²⁵Peking University, Beijing 100871, People's Republic of China
²⁶Seoul National University, Seoul, 151-747 Korea
²⁷Shandong University, Jinan 250100, People's Republic of China
²⁸Shanxi University, Taiyuan 030006, People's Republic of China
²⁹Sichuan University, Chengdu 610064, People's Republic of China
³⁰Soochow University, Suzhou 215006, China
³¹Sun Yat-Sen University, Guangzhou 510275, People's Republic of China
³²The Chinese University of Hong Kong, Shatin, N. T., Hong Kong
³³The University of Hong Kong, Pokfulam, Hong Kong
³⁴Tsinghua University, Beijing 100084, People's Republic of China
³⁵Universitaet Giessen, 35392 Giessen, Germany
³⁶University of Hawaii, Honolulu, Hawaii 96822, USA
³⁷University of Minnesota, Minneapolis, Minnesota 55455, USA
³⁸University of Rochester, Rochester, New York 14627, USA
³⁹University of Science and Technology of China, Hefei 230026, People's Republic of China
⁴⁰University of the Punjab, Lahore-54590, Pakistan
⁴¹University of Turin and INFN, Turin, Italy
⁴²Wuhan University, Wuhan 430072, People's Republic of China
⁴³Zhejiang University, Hangzhou 310027, People's Republic of China
⁴⁴Zhengzhou University, Zhengzhou 450001, People's Republic of China
(Received 14 January 2012; published 3 May 2012)

The decays $J/\psi \rightarrow \gamma\pi^+\pi^-\pi^0$ and $J/\psi \rightarrow \gamma\pi^0\pi^0\pi^0$ are analyzed using a sample of $225 \times 10^6 J/\psi$ events collected with the BESIII detector. The decay of $\eta(1405) \rightarrow f_0(980)\pi^0$ with a large isospin violation is observed for the first time. The width of the $f_0(980)$ observed in the dipion mass spectra is anomalously narrower than the world average. Decay rates for three-pion decays of the η' are also measured precisely.

DOI: 10.1103/PhysRevLett.108.182001

PACS numbers: 13.25.Gv, 12.38.Qk, 14.40.Be

A state near $1440 \text{ MeV}/c^2$ was discovered in $p\bar{p}$ annihilation at rest decaying to $\eta\pi^+\pi^-$ and was subsequently observed decaying to $K\bar{K}\pi$ [1]. Considerable theoretical and experimental efforts have since been devoted to understand its nature. It was proposed to be a candidate for a pseudoscalar glueball [2,3]; the measured mass, however, is much lower than that obtained from lattice QCD calculations, which is above $2 \text{ GeV}/c^2$ [4]. Later, experiments produced evidence that this state was really two different pseudoscalar states, the $\eta(1405)$ and the $\eta(1475)$. The former has large couplings to $a_0(980)\pi$ and $K\bar{K}\pi$, while the latter mainly couples to $K^*\bar{K}$. A detailed review of the experimental situation can be found in Ref. [5].

The nature of the well-established light scalars $f_0(980)$ and $a_0(980)$ is also a matter of controversy. It is not clear whether they belong to the light scalar meson nonet or are

examples of mesons beyond the naive quark model (e.g., tetra-quark states, hybrids, or $K\bar{K}$ molecules) [6–11]. The possibility of mixing between the $f_0(980)$ and $a_0(980)$ was suggested long ago, and its measurement sheds light on the nature of these two resonances [12–17].

The three-pion decays of the η' have garnered attention because their branching ratios (Br) can probe isospin breaking [18,19]. The ratios of the branching ratios [$r_{\pm} \equiv \text{Br}(\eta' \rightarrow \pi^+\pi^-\pi^0)/\text{Br}(\eta' \rightarrow \pi^+\pi^-\eta)$ and $r_0 \equiv \text{Br}(\eta' \rightarrow 3\pi^0)/\text{Br}(\eta' \rightarrow \pi^0\pi^0\eta)$] are related to the strange quark mass and SU(3) breaking [18].

In this Letter, we present the results of a study of $J/\psi \rightarrow \gamma\pi^+\pi^-\pi^0$ and $J/\psi \rightarrow \gamma\pi^0\pi^0\pi^0$. A single structure around $1.4 \text{ GeV}/c^2$ in the $\pi^+\pi^-\pi^0$ ($\pi^0\pi^0\pi^0$) mass spectrum is observed, associated with a narrow structure around $980 \text{ MeV}/c^2$ in the $\pi^+\pi^-$ ($\pi^0\pi^0$) mass spectrum. This

analysis is based on a sample of $(225.2 \pm 2.8) \times 10^6 J/\psi$ events [20] accumulated in the Beijing Spectrometer (BESIII) [21] operating at the Beijing Electron-Positron Collider (BEPCII) [22].

BEPCII is a double-ring e^+e^- collider designed to provide e^+e^- collisions with a peak luminosity of $10^{33} \text{ cm}^{-2} \text{ s}^{-1}$ at a beam current of 0.93 A. The cylindrical core of the BESIII detector consists of a helium-based main drift chamber (MDC), a plastic scintillator time-of-flight system (TOF), and a CsI(Tl) electromagnetic calorimeter (EMC), which are all enclosed in a superconducting solenoidal magnet providing a 1.0 T magnetic field. The solenoid is supported by an octagonal flux-return yoke with resistive plate counter muon identifier modules interleaved with steel. The acceptance of charged particles and photons is 93% over 4π stereo angle, and the charged-particle momentum and photon energy resolutions at 1 GeV are 0.5% and 2.5%, respectively. The BESIII detector is modeled with a Monte Carlo (MC) simulation based on GEANT4 [23,24].

The charged-particle tracks in the polar angle range $|\cos\theta| < 0.93$ are reconstructed from hits in the MDC. Tracks that extrapolate to be within 20 cm of the interaction point in the beam direction and 2 cm in the plane perpendicular to the beam are selected. The TOF and dE/dx information are combined to form particle identification confidence levels for the π , K , and p hypotheses; each track is assigned to the particle type that corresponds to the hypothesis with the highest confidence level. Photon candidates are required to have at least 25 and 50 MeV of energy in the EMC regions $|\cos\theta| < 0.8$ and $0.86 < |\cos\theta| < 0.92$, respectively, and be separated from all charged tracks by more than 10° .

For $J/\psi \rightarrow \gamma\pi^+\pi^-\pi^0$, the candidate events are required to have two oppositely charged tracks identified as pions and at least three photon candidates. A four-constraint (4C) energy-momentum conserving kinematic fit is performed to the $\gamma\gamma\gamma\pi^+\pi^-$ hypothesis, and $\chi_{4C}^2 < 30$ is required. For events with more than three photon candidates, the combination with the smallest χ^2 is retained. To reject possible background events with two or four photons in the final state, the 4C-fit probability for an assignment of the $J/\psi \rightarrow \pi^+\pi^-\gamma\gamma\gamma$ channel must be larger than that of the $J/\psi \rightarrow \pi^+\pi^-\gamma\gamma$ and the $J/\psi \rightarrow \pi^+\pi^-\gamma\gamma\gamma\gamma$ channels. The π^0 candidates are selected by requiring $|M_{\gamma\gamma} - m_{\pi^0}| < 0.015 \text{ GeV}/c^2$. Events with $|M_{\gamma\pi^0} - m_\omega| < 0.05 \text{ GeV}/c^2$ are rejected to suppress the background from $J/\psi \rightarrow \omega\pi^+\pi^-$.

For $J/\psi \rightarrow \gamma 3\pi^0$, the candidate events are required to have no charged track. The $\pi^0 \rightarrow \gamma\gamma$ candidates are formed from pairs of photon candidates that are kinematically fit to the π^0 mass, and the χ^2 from the kinematic fit with 1° of freedom are required to be less than 25. True π^0 mesons decay isotropically in the π^0 rest frame, and their decay distributions are flat, contrary to π^0 candidates

originating from wrong photon combinations. To remove wrong photon combinations, the decay angle, defined as the polar angle of a photon in the π^0 rest frame, is required to satisfy $|\cos\theta_{\text{decay}}| < 0.95$. Events with at least seven and less than nine photons, which form at least three distinct π^0 candidates, are selected. A 7C kinematic fit is performed to the $J/\psi \rightarrow \gamma 3\pi^0$ hypothesis (constraints are the 4-momentum of J/ψ and the three π^0 masses), and $\chi_{7C}^2 < 60$ is required. If there is more than one combination, the combination with the smallest χ_{7C}^2 is retained. Events with $|M_{\gamma\pi^0} - m_\omega| < 0.05 \text{ GeV}/c^2$ are rejected to suppress the background from $J/\psi \rightarrow \omega\pi^0\pi^0$.

The distributions of the selected events in the $M_{\pi^+\pi^-\pi^0} - M_{\pi^+\pi^-}$ and $M_{\pi^0\pi^0\pi^0} - M_{\pi^0\pi^0}$ planes are shown in Figs. 1(a) and 1(b), respectively. The clusters corresponding to $\eta \rightarrow 3\pi$, $\eta' \rightarrow 3\pi$, and $\eta(1405) \rightarrow f_0(980)\pi^0$ can be clearly discerned; the ω signal is also evident in Fig. 1(a), which mainly comes from the background channel $J/\psi \rightarrow \omega\pi^0$, while it is not observed in the neutral channel, as expected from charge conjugation symmetry.

To confirm that the apparent signal for $\eta(1405) \rightarrow f_0(980)\pi^0$ is not caused by background events, we perform a study with an inclusive MC sample of $2.25 \times 10^8 J/\psi$ events generated according to the Lund-Charm model [25] and the Particle Data Group (PDG) decay tables [26]. After the same event selection as above, neither $\eta(1405)$ nor $f_0(980)$ are seen in the mass spectra. Non- $f_0(980)$ or non- $\eta(1405)$ processes are studied using the $f_0(980)$ sidebands ($0.88 \text{ GeV}/c^2 < M_{\pi^+\pi^-(\pi^0\pi^0)} < 0.93 \text{ GeV}/c^2$ and $1.05 \text{ GeV}/c^2 < M_{\pi^+\pi^-(\pi^0\pi^0)} < 1.10 \text{ GeV}/c^2$) or the $\eta(1405)$ sidebands ($1.15 \text{ GeV}/c^2 < M_{\pi^+\pi^-\pi^0(\pi^0\pi^0\pi^0)} < 1.25 \text{ GeV}/c^2$ and $1.55 \text{ GeV}/c^2 < M_{\pi^+\pi^-\pi^0(\pi^0\pi^0\pi^0)} < 1.65 \text{ GeV}/c^2$). No peaking structures are observed.

Figures 2(a) and 2(b) show the $\pi^+\pi^-$ and $\pi^0\pi^0$ mass spectra with the requirement $1.3 \text{ GeV}/c^2 < M_{\pi^+\pi^-\pi^0(3\pi^0)} < 1.5 \text{ GeV}/c^2$. A fit is performed to the $\pi^+\pi^-$ mass spectrum with the $f_0(980)$ signal parameterized by a Breit-Wigner function convolved with a Gaussian mass resolution function plus a second-order Chebychev polynomial background function. The mass, width, and number of events of the $f_0(980)$ obtained from the fit are $m = 989.9 \pm 0.4 \text{ MeV}/c^2$,

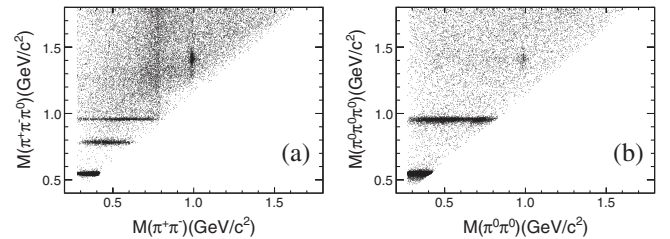


FIG. 1. (a) Scatter plot of $M_{\pi^+\pi^-\pi^0}$ versus $M_{\pi^+\pi^-}$. (b) Scatter plot of $M_{\pi^0\pi^0\pi^0}$ versus $M_{\pi^0\pi^0}$ (3 entries per event).

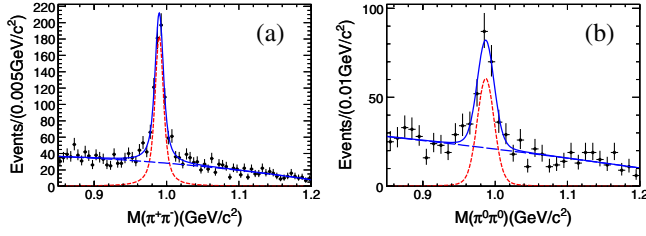


FIG. 2 (color online). The $\pi^+\pi^-$ and $\pi^0\pi^0$ invariant mass spectra with $\pi^+\pi^-\pi^0(3\pi^0)$ in the $\eta(1405)$ mass region. The solid curve is the result of the fit described in the text. The dotted curve is the $f_0(980)$ signal. The dashed curve denotes the background polynomial.

$\Gamma = 9.5 \pm 1.1 \text{ MeV}/c^2$, and $N = 706 \pm 41$, respectively. A fit to the $\pi^0\pi^0$ mass spectrum, shown in Fig. 2(b), is performed in a similar fashion. The mass, width, and number of events of the $f_0(980)$ obtained from the fit are $m = 987.0 \pm 1.4 \text{ MeV}/c^2$, $\Gamma = 4.6 \pm 5.1 \text{ MeV}/c^2$ (less than $11.8 \text{ MeV}/c^2$ at 90% C.L.) and $N = 190 \pm 30$, respectively. The measured width of the $f_0(980)$ is much narrower than the world average.

Figures 3(a) and 3(b) show the $\pi^+\pi^-\pi^0$ and $\pi^0\pi^0\pi^0$ mass spectra where $\pi^+\pi^-(\pi^0\pi^0)$ is in the $f_0(980)$ mass region ($0.94 \text{ GeV}/c^2 < M_{\pi^+\pi^-(\pi^0\pi^0)} < 1.04 \text{ GeV}/c^2$). In addition to the $\eta(1405)$, there is an enhancement at $1.3 \text{ GeV}/c^2$. A fit is performed to the $\pi^+\pi^-\pi^0$ mass spectrum. The two peaks are parametrized by efficiency-corrected Breit-Wigner functions convolved with a Gaussian resolution function. The mass and width of the

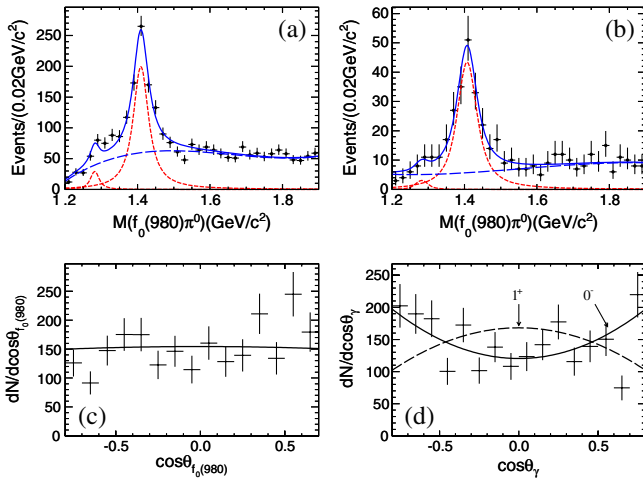


FIG. 3 (color online). Results of the fit to (a) the $f_0(980) \times (\pi^+\pi^-)\pi^0$ and (b) $f_0(980)(\pi^0\pi^0)\pi^0$ invariant mass spectra. The solid curve is the result of the fit described in the text. The dotted curve is the $f_1(1285)/\eta(1295)$ and $\eta(1405)$ signal. The dashed curves denote the background polynomial. Angular distributions of the signal include efficiency corrections. (c) The $\cos\theta_{f_0(980)}$ distribution. The fitting result of $\cos\theta_{f_0(980)}$ is $|\alpha|^2 = 2.10 \pm 0.26$. (d) The $\cos\theta_\gamma$ distribution. The solid line is the prediction for the $J^P = 0^-$ hypothesis, and the dashed line is the prediction for the $J^P = 1^+$ hypothesis with $|\alpha|^2 = 2.10$.

small enhancement are fixed to PDG values of $f_1(1285)$ [26]. The background is described by a third-order Chebychev polynomial with shape parameters determined from a simultaneous fit to the $\pi^+\pi^-\pi^0$ mass spectrum while the $\pi^+\pi^-$ invariant mass is found in the $f_0(980)$ sidebands. The normalization of each component is allowed to float. The masses, widths, number of events, efficiencies, and the product branching ratios of the $\eta(1405)$ and the possible $f_1(1285)/\eta(1295)$ contribution are listed in Table I. The statistical significance of the $\eta(1405)$ is determined by the change of the fit likelihood $-2\ln L$ obtained from the fits with and without the assumption of the $\eta(1405)$ and is found to be well above 10σ . The significance of the potential $f_1(1285)/\eta(1295)$ contribution is determined to be 3.7σ . A fit to the $\pi^0\pi^0\pi^0$ mass spectrum is performed in a similar fashion, shown in Fig. 3(b). The significance of the $\eta(1405)$ is determined to be larger than 10σ . For a possible $f_1(1285)/\eta(1295)$ contribution, the significance is only 1.2σ , and we derive an upper limit on the branching ratio at the 90% C.L. using the Bayesian method.

An angular-distribution analysis is performed with the selected $J/\psi \rightarrow \gamma\eta(1405) \rightarrow \gamma f_0(980)\pi^0 \rightarrow \gamma\pi^+\pi^-\pi^0$ events. Backgrounds are subtracted using the $f_0(980)$ sideband events. For radiative J/ψ decays to a $J^P = 0^-$ meson, the polar angle θ_γ of the photon in the J/ψ center-of-mass system should be distributed according to $1 + \cos^2\theta_\gamma$. In the case of a $J^P = 1^+$ meson, the distributions $\frac{d\sigma}{d\cos\theta_\gamma} \sim 1 + 2|\alpha|^2 + (1 - 2|\alpha|^2)\cos^2\theta_\gamma$ and $\frac{d\sigma}{d\cos\theta_{f_0(980)}} \sim 2 + (|\alpha|^2 - 2)\sin^2\theta_{f_0(980)}$ are expected, where $\theta_{f_0(980)}$ is the polar angle of $f_0(980)$ in the helicity frame of $\eta(1405)$, α is the ratio of helicity 1 to helicity 0. For the $J^P = 1^+$ assumption, $|\alpha|^2$ is determined to be 2.10 ± 0.26 from a fit to $\cos\theta_{f_0(980)}$ [Fig. 3(c)]. The fitting $\chi^2/\text{number of degrees of freedom}$ of Fig. 3(d) with $|\alpha|^2 = 2.10$ is $59.4/15$. For the $J^P = 0^-$ assumption, the fitting $\chi^2/\text{number of degrees of freedom}$ of Fig. 3(d) is $38.4/15$. Comparing the probability of 1^+ hypothesis to 0^- hypothesis, the ratio of the probabilities is 4.1×10^{-4} . The fitting results favor the $J^P = 0^-$ assignment of the $\eta(1405)$.

Figures 4(a) and 4(b) show the $\pi^+\pi^-\pi^0$ and $\pi^0\pi^0\pi^0$ mass spectra in the η' region. A fit is performed to the $\pi^+\pi^-\pi^0$ mass spectrum, shown in Fig. 4(a). The shape of the η' is obtained from MC simulation and the mass and width of the η' are fixed to its PDG values [26]. The shape of the peaking backgrounds [$J/\psi \rightarrow \gamma\eta' \rightarrow \gamma\gamma\rho^0(\pi^+\pi^-)$ and $J/\psi \rightarrow \gamma\eta' \rightarrow \gamma\gamma\omega(\pi^+\pi^-\pi^0)$] is from exclusive MC samples with predicted background levels of 361 ± 32 and 32 ± 6 events, normalized by branching ratios in the PDG [26] and fixed in the fit. The error on the number of events is estimated by changing the normalization by 1 standard deviation from the PDG value. A second-order Chebychev polynomial is used to describe the sum of other nonpeaking backgrounds.

TABLE I. Summary of measurements of the masses, widths, number of events, the MC efficiencies (ϵ) and the product branching ratios of $\text{Br}(J/\psi \rightarrow \gamma X) \times \text{Br}(X \rightarrow \pi^0 f_0(980)) \times \text{Br}(f_0(980) \rightarrow \pi\pi)$ and the decay branching ratios of $\text{Br}(Y \rightarrow 3\pi)$ for the $\pi^+ \pi^- \pi^0$ and $\pi^0 \pi^0 \pi^0$ channels, where X represents $\eta(1405)$ and the possible $f_1(1285)/\eta(1295)$ contribution, Y represents η' . Here for the branching ratios, the first errors are statistical and the second ones are systematic.

Resonance	$M(\text{MeV}/c^2)$	$\Gamma(\text{MeV}/c^2)$	N_{event}	$\epsilon(\%)$	Branching ratios
$\eta(1405)(\pi^+ \pi^- \pi^0)$	1409.0 ± 1.7	48.3 ± 5.2	743 ± 56	22.20 ± 0.21	$(1.50 \pm 0.11 \pm 0.11) \times 10^{-5}$
$\eta(1405)(\pi^0 \pi^0 \pi^0)$	1407.0 ± 3.5	55.0 ± 11.0	198 ± 23	12.83 ± 0.11	$(7.10 \pm 0.82 \pm 0.72) \times 10^{-6}$
$f_1(1285)/\eta(1295)(\pi^+ \pi^- \pi^0)$	fixed	fixed	60 ± 18	26.99 ± 0.23	$(9.99 \pm 3.00 \pm 1.03) \times 10^{-7}$
$f_1(1285)/\eta(1295)(\pi^0 \pi^0 \pi^0)$	fixed	fixed	23	16.75 ± 0.13	$< 7.11 \times 10^{-7}$
$\eta'(\pi^+ \pi^- \pi^0)$	fixed	fixed	1014 ± 39	22.52 ± 0.19	$(3.83 \pm 0.15 \pm 0.39) \times 10^{-3}$
$\eta'(\pi^0 \pi^0 \pi^0)$	fixed	fixed	309 ± 19	7.57 ± 0.08	$(3.56 \pm 0.22 \pm 0.34) \times 10^{-3}$

For $\eta' \rightarrow \pi^0 \pi^0 \pi^0$, $\chi^2(\gamma \pi^0 \pi^0 \pi^0) < \chi^2(\gamma \eta \pi^0 \pi^0)$ and $|M_{\gamma\gamma} - m_{\eta}| > 0.03 \text{ GeV}/c^2$ are additionally required to remove background events from $\eta' \rightarrow \eta \pi^0 \pi^0$. A fit to the $\pi^0 \pi^0 \pi^0$ mass spectrum is performed as shown in Fig. 4(b). The shapes of the η' and nonpeaking backgrounds are described analogously to the charged mode. The efficiencies and the product branching ratios for the η' obtained from the fit are also listed in Table I. From our measurement and the world average values for branching ratios of $\eta' \rightarrow \eta \pi \pi$ [26], we determine $r_{\pm} = (8.87 \pm 0.98) \times 10^{-3}$ and $r_0 = (16.41 \pm 1.94) \times 10^{-3}$.

The systematic uncertainties on the signal yield arise from fit ranges, signal shapes, and background estimation. In detail, for the $\eta(1405)$ signal, the signal shape is given by a Breit-Wigner function with floating mass and width. Its uncertainties are estimated by fixing the mass and width of the $\eta(1405)$ to the world average values. For the possible $f_1(1285)/\eta(1295)$ contribution and η' signal, uncertainties are estimated by changing their mass and width by 1 standard deviation from the PDG values. The uncertainty due to the assumed background shape for the $\eta(1405)$ and the $f_1(1285)/\eta(1295)$ has been estimated using different $f_0(980)$ sidebands, while that of the η' is studied using different order polynomials. For $\eta' \rightarrow \pi^+ \pi^- \pi^0$, the uncertainty of the peaking background is estimated by using the shape from the π^0 sidebands instead of using the shape from exclusive MC samples. The systematic errors on the branching ratio measurements are also subject to system-

atic uncertainties in the number of J/ψ events [20], the intermediate branching ratios [26], the data-MC difference in the π tracking efficiency, the photon detection efficiency, particle identification, the kinematic fit, and the π^0 selection. Combined in quadrature with the uncertainty from the mass spectrum fitting, the systematic errors on the product branching ratios of the $\eta(1405)$, $f_1(1285)/\eta(1295)$, and η' are summarized in Table I.

The $\eta(1405) \rightarrow f_0(980) \pi^0$ signal could arise via $\eta(1405) \rightarrow a_0^0(980) \pi^0$ and $a_0^0(980) - f_0(980)$ mixing. Using the branching ratio of $J/\psi \rightarrow \gamma \eta(1405) \rightarrow \gamma \eta \pi^+ \pi^-$ and the largest PDG value of $\Gamma(\eta(1405) \rightarrow a_0(980) \pi)/\Gamma(\eta(1405) \rightarrow \eta \pi \pi)$, $\text{Br}(J/\psi \rightarrow \gamma \eta(1405) \rightarrow \gamma a_0^0(980) \pi^0 \rightarrow \gamma \pi^0 \eta \pi^0) = (8.40 \pm 1.75) \times 10^{-5}$. The $a_0^0(980) - f_0(980)$ mixing intensity [$\xi_{af} = \text{Br}(\chi_{c1} \rightarrow f_0(980) \pi^0 \rightarrow \pi^+ \pi^- \pi^0)/\text{Br}(\chi_{c1} \rightarrow a_0^0(980) \pi^0 \rightarrow \eta \pi^0 \pi^0)$] measured at BESIII is less than 1% (90% C.L.) [27]. The branching ratio of $J/\psi \rightarrow \gamma \eta(1405) \rightarrow \gamma a_0^0(980) \pi^0 \rightarrow \gamma f_0(980) \pi^0 \rightarrow \gamma \pi^+ \pi^- \pi^0$ is thus expected to be less than $(8.40 \pm 1.75) \times 10^{-7}$, which is much smaller than the result that we measure. Therefore, $a_0^0(980) - f_0(980)$ mixing alone can not explain the observed branching ratio of $\eta(1405) \rightarrow f_0(980) \pi^0$.

To interpret the anomalously narrow width of $f_0(980)$ and large isospin violation observed in this channel, Wu *et al.* recently proposed that a novel scenario of triangle singularity would play a crucial role in this process [28]. Further theoretical and experimental studies are needed for a better understanding of the underlying dynamics.

In summary, we have studied $J/\psi \rightarrow \gamma 3\pi$ decays. The isospin violating decay $\eta(1405) \rightarrow f_0(980) \pi^0$ is observed for the first time with a statistical significance larger than 10σ in both the charged and neutral modes. According to our measurement, the ratio of $\text{Br}(\eta(1405) \rightarrow f_0(980) \pi^0 \rightarrow \pi^+ \pi^- \pi^0)$ to $\text{Br}(\eta(1405) \rightarrow a_0^0(980) \pi^0 \rightarrow \eta \pi^0 \pi^0)$ is $(17.9 \pm 4.2)\%$ [26,29], which is 1 order of magnitude larger than the $a_0^0(980) - f_0(980)$ mixing intensity (less than 1%) determined at BESIII previously [27]. The measured width of the $f_0(980)$ is anomalously narrower than the world average. There is also evidence for an enhancement at around $1.3 \text{ GeV}/c^2$ [potentially from the $f_1(1285)/\eta(1295)$] seen with a significance of 3.7σ in

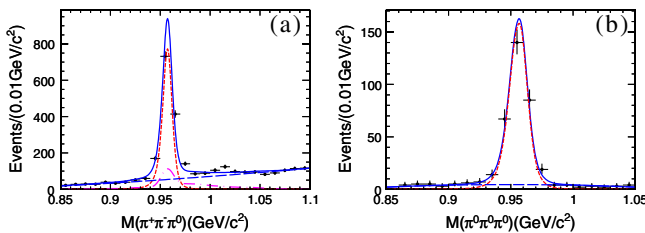


FIG. 4 (color online). Results of the fit to (a) the $\pi^+ \pi^- \pi^0$ and (b) $3\pi^0$ invariant mass spectra. The solid curve is the result of the fit described in the text. The dotted curve is the η' signal. The dashed curves denote the background polynomial. The dash-dotted curve in (a) describes the peaking background.

the charged mode and 1.2σ in the neutral mode. For the decay $\eta' \rightarrow \pi^+ \pi^- \pi^0$, the branching ratio that we measure is consistent with the CLEO-*c* measurement [30], and the precision is improved by a factor of 4. For the decay $\eta' \rightarrow 3\pi^0$, it is 2 times larger than the world average value [26]. Using our new measurement of the decay rates for $\eta' \rightarrow 3\pi$, the values of r_{\pm} and r_0 are more than 4 standard deviations away from both $\pi^0 - \eta$ mixing prediction and the chiral unitary framework prediction [19].

The BESIII Collaboration thanks the staff of BEPCII and the computing center for their hard efforts. Useful discussions with K. T. Chao, S. L. Zhu, and J. J. Wu are acknowledged. This work is supported in part by the Ministry of Science and Technology of China under Contract No. 2009CB825200; National Natural Science Foundation of China (NSFC) under Contracts No. 10625524, No. 10821063, No. 10825524, No. 10835001, No. 10935007, No. 11125525; the Chinese Academy of Sciences (CAS) Large-Scale Scientific Facility Program; CAS under Contracts No. KJCX2-YW-N29, No. KJCX2-YW-N45; 100 Talents Program of CAS; Istituto Nazionale di Fisica Nucleare, Italy; Siberian Branch of Russian Academy of Science, joint project No 32 with CAS; U.S. Department of Energy under Contracts No. DE-FG02-04ER41291, No. DE-FG02-91ER40682, No. DE-FG02-94ER40823; University of Groningen (RuG) and the Helmholtzzentrum fuer Schwerionenforschung GmbH (GSI), Darmstadt; WCU Program of National Research Foundation of Korea under Contract No. R32-2008-000-10155-0.

*Also at the Moscow Institute of Physics and Technology, Moscow, Russia.

†On leave from the Bogolyubov Institute for Theoretical Physics, Kiev, Ukraine.

‡Present address: University of Perugia and INFN, Perugia, Italy.

§Also at the PNPI, Gatchina, Russia.

||Present address: Nagoya University, Nagoya, Japan.

- [1] P. H. Baillon *et al.*, *Nuovo Cimento A* **50**, 393 (1967).
- [2] M. Acciarri *et al.* (L3 Collaboration), *Phys. Lett. B* **501**, 1 (2001).
- [3] L. Faddeev, A. J. Niemi, and U. Wiedner, *Phys. Rev. D* **70**, 114033 (2004).

- [4] G. S. Bali *et al.*, *Phys. Lett. B* **309**, 378 (1993).
- [5] A. Masoni, C. Cicalo, and G. L. Usai, *J. Phys. G* **32**, R293 (2006).
- [6] R. L. Jaffe, *Phys. Rev. D* **15**, 267 (1977).
- [7] N. N. Achasov and V. N. Ivanchenko, *Nucl. Phys.* **B315**, 465 (1989).
- [8] N. N. Achasov and V. V. Gubin, *Phys. Rev. D* **56**, 4084 (1997).
- [9] J. D. Weinstein and N. Isgur, *Phys. Rev. D* **27**, 588 (1983).
- [10] J. D. Weinstein and N. Isgur, *Phys. Rev. D* **41**, 2236 (1990).
- [11] S. Ishida *et al.*, in *Proceedings of the 6th International Conference on Hadron Spectroscopy* (World Scientific, Manchester, United Kingdom, Singapore, 1995), p. 454.
- [12] N. N. Achasov, S. A. Devyanin, and G. N. Shestakov, *Phys. Lett. B* **88**, 367 (1979).
- [13] C. Hanhart, B. Kubis, and J. R. Pelaez, *Phys. Rev. D* **76**, 074028 (2007).
- [14] N. N. Achasov and A. V. Kiselev, *Phys. Lett. B* **534**, 83 (2002).
- [15] B. Kerbikov and F. Tabakin, *Phys. Rev. C* **62**, 064601 (2000).
- [16] N. N. Achasov and G. N. Shestakov, *Phys. Rev. Lett.* **92**, 182001 (2004).
- [17] F. E. Close and A. Kirk, *Phys. Lett. B* **489**, 24 (2000).
- [18] D. J. Gross, S. B. Treiman, and F. Wilczek, *Phys. Rev. D* **19**, 2188 (1979).
- [19] B. Borasoy, U.-G. Meissner, and R. Nissler, *Phys. Lett. B* **643**, 41 (2006).
- [20] M. Ablikim *et al.* (BESIII Collaboration), *Phys. Rev. D* **83**, 012003 (2011).
- [21] M. Ablikim *et al.* (BESIII Collaboration), *Nucl. Instrum. Methods Phys. Res., Sect. A* **614**, 345 (2010).
- [22] J. Z. Bai *et al.* (BES Collaboration), *Nucl. Instrum. Methods Phys. Res., Sect. A* **458**, 627 (2001).
- [23] S. Agostinelli *et al.* (GEANT4 Collaboration), *Nucl. Instrum. Methods Phys. Res., Sect. A* **506**, 250 (2003).
- [24] J. Allison *et al.*, *IEEE Trans. Nucl. Sci.* **53**, 270 (2006).
- [25] R. G. Ping, *Chinese Phys. C* **32**, 599 (2008).
- [26] K. Nakamura *et al.* (Particle Data Group), *J. Phys. G* **37**, 075021 (2010).
- [27] M. Ablikim *et al.* (BESIII Collaboration), *Phys. Rev. D* **83**, 032003 (2011).
- [28] J. J. Wu, X. H. Liu, Q. Zhao, and B. S. Zou, *Phys. Rev. Lett.* **108**, 081803 (2012).
- [29] C. Amsler *et al.* (Crystal Barrel Collaboration), *Phys. Lett. B* **358**, 389 (1995).
- [30] P. Naik *et al.* (CLEO Collaboration), *Phys. Rev. Lett.* **102**, 061801 (2009).